XII International Conference on Computational Plasticity. Fundamentals and Applications
COMPLAS XII
E. Oñate, D.R.J. Owen, D. Peric and B. Suárez (Eds)

LEAD EXTRUSION ANALYSIS BY FINITE VOLUME METHOD

MARCELO M. MARTINS[*], JOSÉ D. BRESSAN[†] AND SÉRGIO T. BUTTON[†]

[*]Centre University – Catholic of Santa Catarina - Campus Centro
Visconde de Taunay 427, 89203-005 Joinville - SC, Brazil
e-mail: marcelo.martins@catolicasc.org.br, web page: http:// http://www.catolicasc.org.br/

[†] Department of Mechanical Engineering
Centre for Technological Science
University of Santa Catarina State (UDESC)
Campus Universitário Prof. Avelino Marcante
Paulo Malschitzki s/n, 89219-710, Joinville - SC, Brazil
Email: dem2jdb@joinville.udesc.br - Web page: http://www.joinville.udesc.br/

[†] Department of Materials Engineering
Faculty of Mechanical Engineering
State University of Campinas (UNICAMP)
Campus Cidade Universitário "Zeferino Vaz"
Mendeleyev 200, 13083-860, Campinas - SP, Brazil
Email: sergio1@fem.unicamp.br - Web page: http://www.fem.unicamp.br/

Key words: Extrusion; Finite Volume Method; MacCormack Method; Manufacturing processes; Lead.

Abstract. Computational numerical simulation is nowadays largely applied in the design and analysis of metal forming process. Extrusion of metals is one main forming process largely applied in the manufacturing of metallic products or parts. Historically, the Finite Element Method has been applied for decades in metal extrusion analysis [4]. However, recently in the academy, there is a trend to use Finite Volume Method: literature suggests that metal flow by extrusion can be analyzed by the flow formulation [1, 2]. Thus, metal flow can be modelled such us an incompressible viscous fluid [2]. This hypothesis can be assumed because extrusion process is an isochoric process. The MacCormack Method is commonly used to simulate compressible fluid flow by the finite volume method [3]. However, metal extrusion and incompressible fluid flow do not present state equations for the evolution of pressure, and therefore, a velocity-pressure coupling method is necessary to obtain a consistent velocity and pressure fields [3]. Present work proposes a new numerical scheme to obtain information about metal flow in the extrusion process, in steady state. The governing equations were discretized by Finite Volume Method, using the Explicit MacCormack Method to structured and collocated mesh. The SIMPLE Method was applied to attain pressure-velocity coupling [3]. These new numerical scheme was applied to forward extrusion process of lead. The incompressible metal extrusion velocity fields achieved faster convergence and a good agreement with analytical and experimental results obtained from literature. The MacCormack Method applied for metals produced consistent results without the need of

artificial viscosity as employed by the compressible flow simulation approaches. Furthermore, the present numerical results also suggest that MacCormack Method and SIMPLE can be applied in the solution of metal forming processes besides the traditional application for compressible fluid flow.

1 INTRODUCTION

In the academic and industrial environment, the numerical simulation is an unquestionable reality. This can be seen by the great number of scientific papers published on journals and conference that treat the theme. In addition, many industries employ commercial codes or code made by their own engineers to analyze projects. In the metal forming area is not different. There are many scientific papers published which treat of metal forming phenomena by numerical simulation.

This is because the computer has increased steadily the processing power, this reality became true since 1950's. Simultaneously, the numerical method applied to solve mathematic equations to governing physics phenomena of metal forming have to be adapted to specific situations. This way, one can highlight the importance of Finite Element Method (FEM) to simulate metal forming process [4].

The FEM was created in 1950's linked with elasticity structural problems. In the next decade, the FEM was applied in metal forming, but at that time it was utilized solid formulation (considering elasto-plastic materials and elasto-viscous-plastic materials). However, this formulation was inadequate to analyse the non-linearities (geometric and material non-linearity) which appeared from these problems [4].

In 1970's, it was developed the flow formulation. In metal forming processes, the flow formulation considers the metal similar to an incompressible viscous fluid. The incompressible viscous fluid was and still is treated numerically by Finite Volume Method (FVM). The flow formulation can be assumed because metal forming processes are isochoric, i.e., constant volume. The flow formulation considers that materials are rigid-elastic-plastic and rigid-viscous-plastic, thus, the elastic deformations are neglected because the high value of plastic deformations in metal forming processes [4].

The FEM is still nowadays the preferential choice to analyse metal forming problems. However, from 1990's there was an increase of interest to use FVM in metal forming problems [2]. This happened because FVM is a method well tested in fluid dynamic and this knowledge will help to understand metal forming phenomena and to create numerical codes which can involve analysis of solid and fluid or interactions between them [4].

The FVM was created in 1970's for solving the limitations of Finite Difference Method (FDM). FVD was the numerical method used in dynamic fluid [6]. Increase utilization of FVM came from its main feature, that is, satisfy the conservations law in global and discrete levels. Thus, it is linked with more consistent physical interpretation. Knowing that, FEM and FDM do not satisfy conservations law in discrete level because they do not work with control volumes but with mesh points [6]. Then, from 1990's appeared, in the literature, a lot of works to simulate numerically metal forming process by FVM and flow formulation [5, 13].

Usually, the parameters used to analyse fluid flow are velocity, temperature and pressure fields. This information gives a good vision about fluid flow behaviour. In metal forming flow

it is necessary to determine these same fields. These information supply quantitative data of metal forming process that help to analyse metal forming process by a qualitative way.

Both fluid flow and metal flow are governed by conservation law equations (mass, momentum and energy). The constitutive equations are different for both cases and they define the material type. The governing equations and the constitutive equations together are necessary information and sufficient to apply a numerical method [3].

When the conservation equations are discretized by FVM using explicit formulation, they generate set of non-linear equations [6]. There are many numerical methods to solve the set of non-linear equations. But, all methods should have a good convergence, stability and accuracy. The MacCormack Method has been highlighted in dynamic fluid applications.

The MacCormack Method is traditionally used in compressible fluid flow in aerodynamics analysis because it smooth discontinuity picks produced by shock waves in these kinds of flows. The main features of MacCormack Method are to have second order accuracy in time and space.

The MacCormack Method still has good results in the treatment of non-linearities of Partial Differential Equations. As metal forming flow are governed by Conservations Differential Equations and considering discontinuity regions in the entrance and outlet deformations zones in direct extrusion process, then, this work proposes to use the MacCormack method to solve the governing equations of metal flow in direct extrusion process [11].

2 MATHEMATICAL MODELLING

2.1 Governing Equations

The mathematical modelling in metal flow of direct extrusion process can be treated by FVM using flow formulation. According [8] metal flow is considered similar to fluid viscous flow. [11] suggests fluid viscous flow can be mathematically represented by mass, momentum and energy conservation equations which are considered below:

$$\frac{\partial \rho}{\partial t} + \nabla \cdot (\rho \boldsymbol{v}) = 0 \tag{1}$$

$$\frac{\partial (\rho \boldsymbol{v})}{\partial t} + \nabla \cdot (\rho \boldsymbol{v}\boldsymbol{v}) = \nabla \cdot \boldsymbol{\sigma} + \rho \boldsymbol{b} \tag{2}$$

$$\frac{\partial (\rho e)}{\partial t} + \nabla \cdot (\rho e \boldsymbol{v}) = \rho r - \nabla \cdot \dot{\boldsymbol{q}} + \rho \boldsymbol{b} \cdot \boldsymbol{v} + \nabla \cdot (\boldsymbol{\sigma} \cdot \boldsymbol{v}) \tag{3}$$

where, ρ is density, $\boldsymbol{v}$ is velocity vector, $\boldsymbol{b}$ are body forces, $\boldsymbol{\sigma}$ is Cauchy stress tensor, $\dot{\boldsymbol{q}}$ is heat flux vector, e is specific energy, r is heat generate and t is the time. Considering Eq. (1), (2) and (3) in cylindrical coordinates for axisymmetric case, these equations can be written in matrix structure in the following form:

$$\frac{\partial \boldsymbol{Q}}{\partial t}+\frac{1}{r}\frac{\partial\left(r\boldsymbol{F}_r\right)}{\partial r}+\frac{\partial \boldsymbol{F}_z}{\partial z}=\boldsymbol{S} \tag{4}$$

where, r is radial coordinate, z is axial coordinate, $\boldsymbol{Q}$, $\boldsymbol{F}_r$, $\boldsymbol{F}_z$ e $\boldsymbol{S}$ are flux vectors that assume the following format:

$$\boldsymbol{Q}=\begin{Bmatrix}\rho\\ \rho v_r\\ \rho v_z\\ \rho cT\end{Bmatrix} \quad \boldsymbol{F}_r=\begin{Bmatrix}\rho v_r\\ \rho v_r^2-\sigma_{rr}\\ \rho v_r v_z-\sigma_{rz}\\ \rho cTv_r+\dot{q}_r\end{Bmatrix} \quad \boldsymbol{F}_z=\begin{Bmatrix}\rho v_z\\ \rho v_z v_r-\sigma_{rz}\\ \rho v_z^2-\sigma_{zz}\\ \rho cTv_z+\dot{q}_z\end{Bmatrix} \quad \boldsymbol{S}=\begin{Bmatrix}0\\ -\dfrac{\sigma_{\theta\theta}}{r}\\ 0\\ \bar{\sigma}.\dot{\bar{\varepsilon}}\end{Bmatrix} \tag{5}$$

being, σ_{rr}, $\sigma_{\theta\theta}$ and σ_{zz} normal components and σ_{rz} is the shear component of Cauchy stress tensor, T is temperature, c is specific heat, $\dot{q}_r$ and $\dot{q}_z$ are flux heat vector, v_r and v_z are velocity vector components, $\bar{\sigma}$ effective stress and $\dot{\bar{\varepsilon}}$ is effective strain rate.

2.2 Plasticity Constitutive Equations

Plasticity constitutive equations are mathematic expressions that govern the material behaviour in mechanical and/or thermal loading by static variable (given by stresses), kinematic (given by displacements, deformations and velocities) and thermal (given by flux thermal and temperature) [7]. Metal constitutive equation for axisymmetric plastic flow is considered to be incompressible, isotropic and rigid-viscous-plastic material. Relation between the stress tensor and the strain rate tensor can be written in the following form:

$$\boldsymbol{\sigma}=-\sigma_m+2\eta\dot{\varepsilon} \tag{6}$$

where, $\boldsymbol{\sigma}$ is the Cauchy stress tensor, $\dot{\varepsilon}$ is strain rate tensor, σ_m is hydrostatic pressure and η is metal viscosity. Hydrostatic pressure inside the solid is calculated by:

$$\sigma_m=\frac{\sigma_{rr}+\sigma_{\theta\theta}+\sigma_{zz}}{3} \tag{7}$$

where, σ_{rr}, $\sigma_{\theta\theta}$ *and* σ_{zz} are principal stresses of the stress tensor. Metal viscosity η is defined by the *Associated Plastic Flow Rule* by equation:

$$\dot{\varepsilon}=\dot{\lambda}\sigma' \tag{8}$$

being σ' the deviatoric tensor and $\dot{\lambda}$ the plastic multiplier. Metal viscosity η can be calculated by the following equation:

$$\eta=\frac{1}{3}\frac{\bar{\sigma}}{\dot{\bar{\varepsilon}}}=\frac{1}{2\dot{\lambda}} \tag{9}$$

where $\bar{\sigma}$ is the effective stress and $\dot{\bar{\varepsilon}}$ is the effective strain rate. The effective strain rate must not assume values less than 10^{-3} to avoid numerical instability.

1 NUMERICAL METHOD

3.1 Finite Volume Method

Considering Eq. (4) and integrating over the control volume given by Figure 1a, using Gauss' Theorem, results in the following equation:

$$\frac{\partial \boldsymbol{Q}_{mn}}{\partial t} = -\frac{1}{V_{mn}}\left\{\frac{1}{r}\left[\left(r\boldsymbol{F}_r \cdot \boldsymbol{s}\right)_{m,n-\frac{1}{2}} + \left(r\boldsymbol{F}_r \cdot \boldsymbol{s}\right)_{m,n+\frac{1}{2}}\right] + \left[\left(\boldsymbol{F}_z \cdot \boldsymbol{s}\right)_{m-\frac{1}{2},n} + \left(\boldsymbol{F}_z \cdot \boldsymbol{s}\right)_{m+\frac{1}{2},n}\right]\right\} + \boldsymbol{S}_{mn} \tag{10}$$

where $\boldsymbol{s}$ is the outward surface vector and V_{mn} is control volume area.

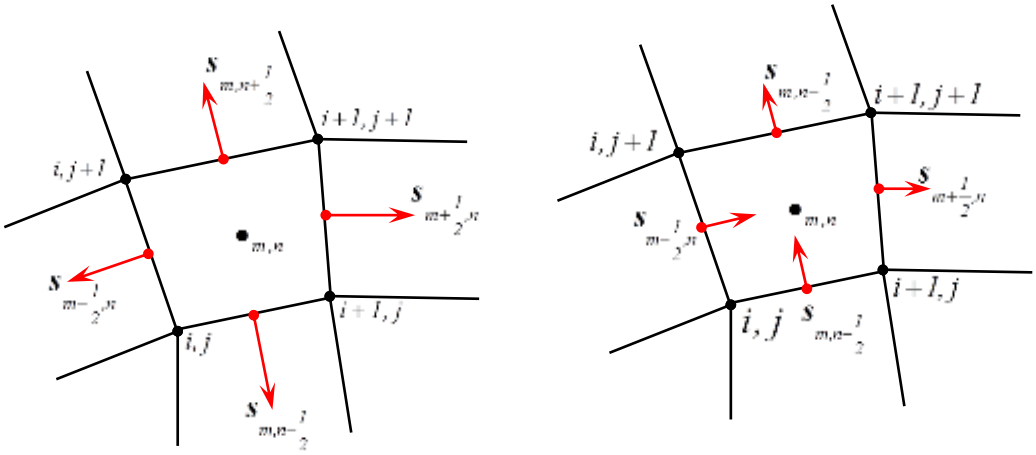

Figure 1. Representation of quadrilateral control volume. (a) Specification of outward vector. (b) Outward vector correction.

3.2 MacCormack Method

Explicit MacCormack scheme was applied in the Eq. (10). This scheme use explicit Euler scheme on time. Considering outward surface vector on the control volume given by Figure 1b, thus, Eq. (11) represents the predictor step, Eq. (12) represents the corrector step and Eq. (13) represents the current step. MacCormack scheme is a pseudo-transient process, where Δt is a virtual time increment to obtain the final converged solution.

$$\underline{\boldsymbol{Q}}_{mn}^{t+1} = \boldsymbol{Q}_{mn}^{t} - \frac{\Delta t}{V_{mn}}\left\{\frac{1}{r}\left[\left(r\boldsymbol{F}_{m,n+1} \cdot \boldsymbol{s}_{m,n+\frac{1}{2}}\right) - \left(r\boldsymbol{F}_{m,n} \cdot \boldsymbol{s}_{m,n-\frac{1}{2}}\right)\right] + \left[\left(\boldsymbol{F}_{m+1,n} \cdot \boldsymbol{s}_{m+\frac{1}{2},n}\right) - \left(\boldsymbol{F}_{m,n} \cdot \boldsymbol{s}_{m-\frac{1}{2},n}\right)\right]\right\}^{t} + \Delta t\, \boldsymbol{S}_{mn}^{t} \tag{11}$$

$$\underline{\underline{\boldsymbol{Q}}}_{mn}^{t+1} = \boldsymbol{Q}_{mn}^{t} - \frac{\Delta t}{V_{mn}}\left\{\frac{1}{r}\left[\left(r\underline{\boldsymbol{F}}_{m,n} \cdot \boldsymbol{s}_{m,n+\frac{1}{2}}\right) - \left(r\underline{\boldsymbol{F}}_{m,n-1} \cdot \boldsymbol{s}_{m,n-\frac{1}{2}}\right)\right] + \left[\left(\underline{\boldsymbol{F}}_{m,n} \cdot \boldsymbol{s}_{m+\frac{1}{2},n}\right) - \left(\underline{\boldsymbol{F}}_{m-1,n} \cdot \boldsymbol{s}_{m-\frac{1}{2},n}\right)\right]\right\}^{t} + \Delta t\, \boldsymbol{S}_{mn}^{t} \tag{12}$$

$$\boldsymbol{Q}_{mn}^{t+1} = \frac{1}{2}\left(\underline{\boldsymbol{Q}}_{mn}^{t+1} + \underline{\underline{\boldsymbol{Q}}}_{mn}^{t+1}\right) \tag{13}$$

where, t is current time, $t+1$ is next time step, Δt is a virtual time step, $\underline{Q}_{mn}^{t+1}$ is predictor step, $\underline{\underline{Q}}_{mn}^{t+1}$ is corrector step and Q_{mn}^{t+1} is current step. The flux vector $\boldsymbol{F}$, inside Eq. (11) and Eq. (12), must be discretized in correct way to ensure the main feature of MacCormack Method: second order accuracy in time and space [11].

3.3 Velocity-Pressure Coupling

The SIMPLE Method was applied to obtain coupling velocity-pressure in the numerical scheme developed in this work. The SIMPLE Method makes the coupling by corrections in both variables, i.e., velocity and pressure. To attain this, the method utilizes the following equations:

$$p = p_0 + p' \tag{14}$$

$$\boldsymbol{v} = \boldsymbol{v}_0 + \boldsymbol{v}' \tag{15}$$

the variables p and $\boldsymbol{v}$ are current values of pressure and velocity vector, respectively, the variables p_0 and $\boldsymbol{v}_0$ are estimated pressure and velocity vectors and the variables p' and $\boldsymbol{v}'$ are corrections of each variables. According [6], the corrections equations at discretized volume are given by:

$$(v_z)'_e = (v_z)^*_e - A\left(\frac{p'_E - p'_P}{\delta z_e}\right) \tag{16}$$

$$(v_z)'_w = (v_z)^*_w - A\left(\frac{p'_P - p'_W}{\delta z_w}\right) \tag{17}$$

$$(v_r)'_n = (v_r)^*_n - A\left(\frac{p'_N - p'_P}{\delta r_n}\right) \tag{18}$$

$$(v_r)'_s = (v_r)^*_s - A\left(\frac{p'_P - p'_S}{\delta r_s}\right) \tag{19}$$

lowercase subscripts represent face position of control volumes and upper case subscripts represents the centre position of control volumes, according to Figure 2. The term A is defined as the quotient between fictitious time step and density, according [11]. The velocities v_r and v_z must be considered on the faces of control volumes, i.e., the velocities must be dislocated from control volume centre to the control volume faces in order to have the ideal coupling between velocity and pressure fields. To this process, it was used the Momentum Interpolation Method [10]. [6] suggests the following correction equation to pressure or the Poisson equation that calculate p':

$$p'_P = \left(A_E p'_E + A_W p'_W + A_N p'_N + A_S p'_S + B\right) / A_P \tag{20}$$

where:

$$A_P = A_E + A_W + A_N + A_S$$

$$A_E = \frac{r\rho A\Delta t\Delta r}{\delta z_e} \qquad A_W = \frac{r\rho A\Delta t\Delta r}{\delta z_w} \qquad A_N = \frac{r_n\rho A\Delta t\Delta z}{\delta r_n} \qquad A_S = \frac{r_s\rho A\Delta t\Delta z}{\delta r_s} \tag{21}$$

$$B = \left[(v_z)_w^* - (v_z)_e^*\right]\rho r\Delta r + \left[r_s(v_r)_s^* - r_n(v_r)_n^*\right]\rho\Delta z \qquad A = \frac{\Delta t}{\rho}$$

being r_n the radius on *n* face and r_s is radius on *s* face of control volume.

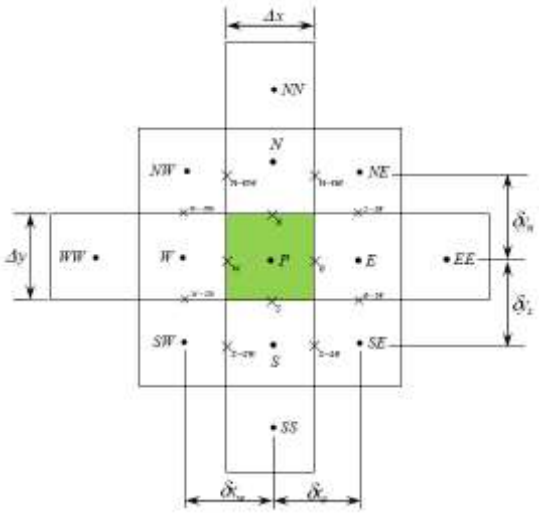

Figure 2. Representation of main control volume and its neighbours [14].

3.4 Boundary Conditions

The boundary conditions were imposed over the control volume faces. These boundary conditions were imposed using the scheme called *"Ghost Volume"*. In these ghost volumes it can be applied boundary condition of *"Dirichlet Kind"* and *"Neumann kind"*. According [6, 15] the boundary conditions applied for metal flow in direct extrusion analysis should be imposed in this way, being control volumes walls represented by Figure 3:

- **Inlet:** the velocity field should be prescribed and pressure should have zero gradient.
- **Outlet:** the velocity should have zero gradient and pressure should be prescribed.
- **Symmetry line:** should be prescribed zero gradients for normal surface gradient and parallel surface components should use domain values.
- **Solid Wall:** as solid wall is interface between material-die, it should consider friction model. The friction model used was Coulomb Friction which can be represented by:

$$\tau_{nt} = \mu\sigma_n \tag{22}$$

where, τ_{nt} is friction stress, μ is Coulomb coefficient and σ_n is contact normal stress.

4 RESULTS

4.1 Case Description

The analysed metal flow in this work treats lead direct extrusion process with die geometry described in reference [1] and that is shown in Figure 3. Where, inlet radius, outlet

radius and die slope of 15°, define a deformation degree equal to 25%. Figure 3 shows the mesh used in the simulations, with 1463 quadrilateral volumes. The material used was considered rigid-perfect-plastic, being Coulomb friction coefficient in a range from zero to 0.5 and applied in the conical die region. Others parameters of direct extrusion process and material involved are presented in Table 1.

Table 1 – Material properties and process parameters of lead direct extrusion employed in the present numerical simulation.

Parameters	**Values**
Yield Strength (σ_Y)	14 (Mpa)
Deformation (ε)	25 %
Initial Velocity (V_0)	1 (mm . s^{-1})
Initial Strain Rate ($\dot{\varepsilon}_0$)	0,9 (s^{-1})
Maximum Coulomb Friction Coefficient (μ)	0,5
Time Step (Δt)	10^{-15} (s)

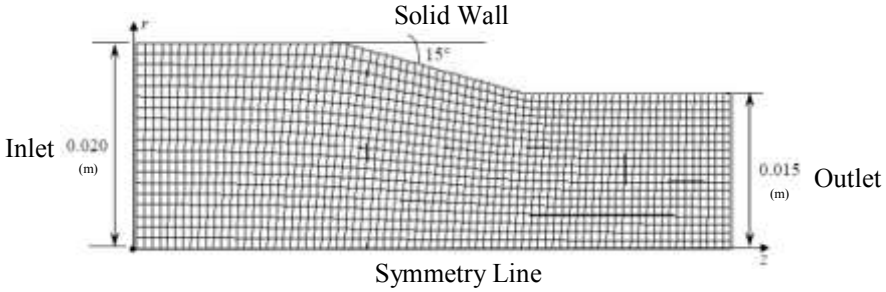

Figure 3. Geometric representation of lead extrusion die, mesh with 1463 volumes.

4.2 Discussion of Results

The numerical results obtained from the numerical scheme presented in this work were compared with the analytical results obtained from Upper Bound Method and other numerical results obtained from literature. The Upper Bound Method employed in this work is presented in [8, 9, 12]. The numerical results from literature are presented in the paper [1].

Figure 4a show a comparison between the results of radial analytical velocity ($v_{r\_analytic}$, generate by Upper Bound Method) and radial numerical velocity ($v_{r\_numeric}$, generate by present numerical scheme). As can be seen the values and contours are in good agreement. Figure 4b show a comparison between the results of axial analytical velocity ($v_{z\_analytic}$, generate by Upper Bound Method) and axial numerical velocity ($v_{z\_analytic}$, generate by present numerical scheme). Again, the results of values and contours are in good agreement.

Figure 5a is showing a comparison between axial numerical velocity contours (Vz) of present work and axial numerical velocity contours (Vz) presented in [1]. It can noticed that values and contours are in good agreement. In the Figure 5b is showed a comparison between

radial numerical velocity contours (*Vr*) of present work and radial numerical velocity contours (*Vr*) presented in [1]. Again, the radial numerical velocity results are in good agreement, but the contours have some differences. These differences can be assigned by different way that was applied Coulomb friction. In the present work, Coulomb´s friction coefficient used the normal pressure at boundary while the paper by [1] employed the hydrostatic pressure.

Figure 6a presents pressure contours, where, it can be observed that there is a compression region at the conical die region, close to material-die interface. The Figure 6b show effective strain rate contours. It can be seen that the biggest effective strain rate arise at conical region close to material-die interface. Figure 6c is showing the effective stress contours. Where, it can be observed rigid regions of material during direct extrusion process.

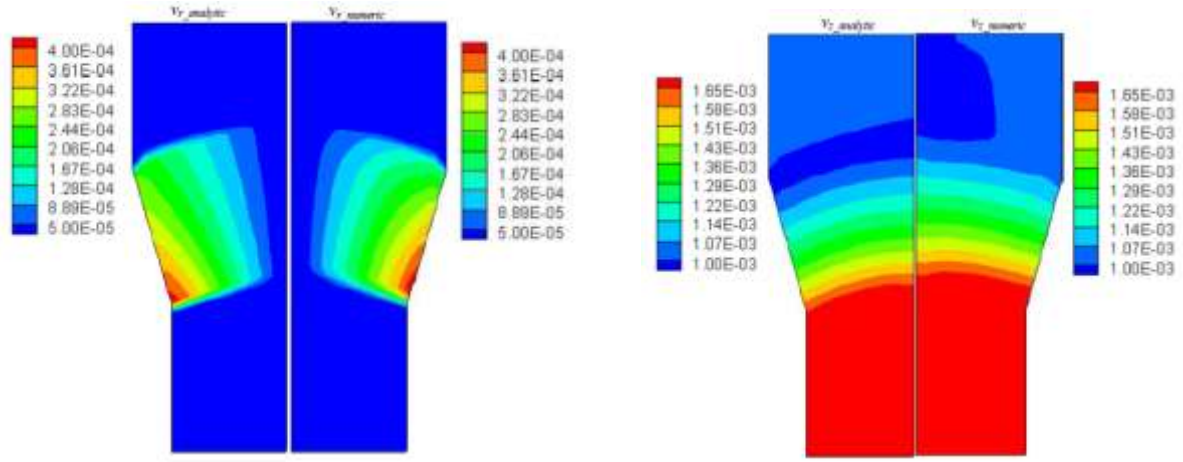

(a) (b)

Figure 4. (a) Comparison between radial analytical velocity contour ($v_{r\_analytic}$) and radial numerical velocity contour ($v_{r\_numeric}$), for no friction direct extrusion. (b) Comparison between axial analytical velocity contour ($v_{z\_analytic}$) and axial numerical velocity contour ($v_{z\_numérica}$), for no friction direct extrusion.

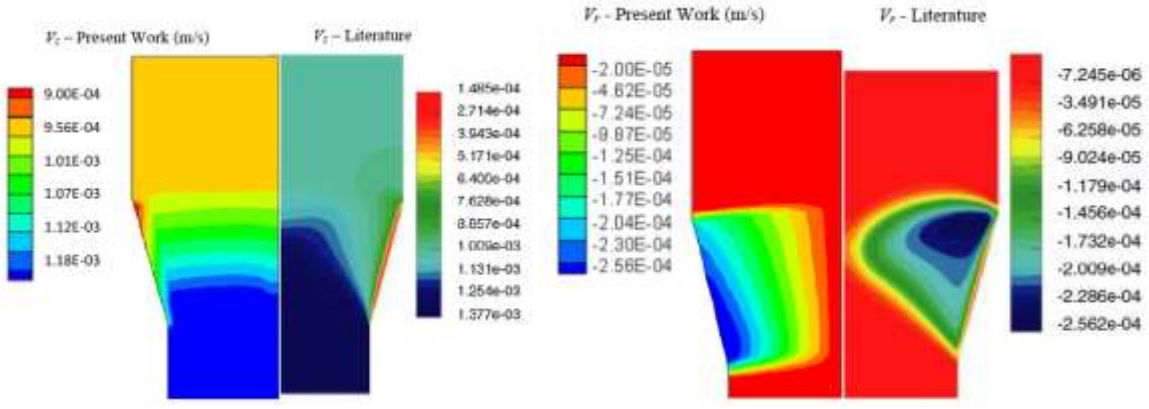

(a) (b)

Figure 5. (a) Comparison between axial numerical velocity contour (V_z) of present work and axial numerical velocity contour presented by [1]. (b) Comparison between radial numerical velocity contour (Vr) of present work and radial numerical velocity contour presented by [1].

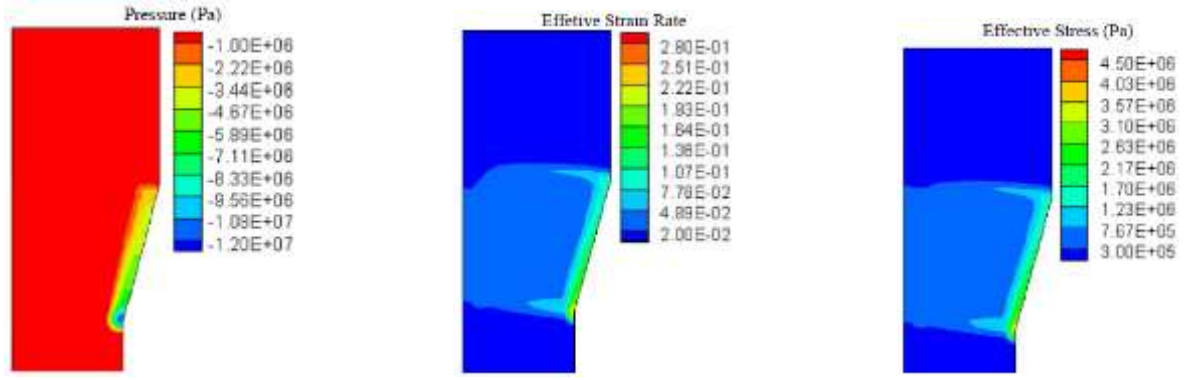

(a) (b) (c)

Figure 6. (a) Pressure contours calculated by present work. (b) Effective strain rate contours calculated by present work. (c) Effective stress contours calculated by present work.

5 CONCLUSIONS

The present numerical scheme applied in metal flow of lead direct extrusion process allowed to obtain the following conclusions:

- Numerical results was calculated by the present finite volume numerical scheme without artificial viscosity;
- Numerical scheme presented is explicit, then it is conditionally stable because it was used a time step equal 10^{-15} to satisfy CFL condition;
- the axial velocity increased its magnitude at entrance of conical die region, being the biggest axial velocity achieved at the outlet die region;
- at the conical region of material-die interface occurred the biggest pressure magnitude and the biggest effective strain rate;
- numerical scheme convergence was achieved, for axial and radial velocity and pressure, with about 20.000 iterations;
- FVM with MacCormack Method together flow formulation was able to produce good results for metal flow of lead direct extrusion process;
- MacCormack Method besides to be applied in compressible flow analysis, as proved by the literature, can also be applied in metal flow in direct extrusion.

6 ACKNOWLEDGEMENTS

The authors would like to thank the support of The National Council for Scientific and Technological Development (CNPq) – Brazil, State University of Campinas (UNICAMP) – Brazil, University of Santa Catarina State (UDESC) – Brazil and University Centre – Catholic of Santa Catarina – Brazil.

7 REFERENCES

[1] Basic, H. and Demirdzic, I. and Muzaferija, S. Finite volume method for simulation of extrusion processes. *Inter. Journ. for Num. Meth. in Eng.* (2005) 62: 475–494.

[2] Demirdzic, I. and Dzaferovic, E. and Ivankovic, A. Finite-Volume Approach to Thermoviscoelasticity. *Num.Heat Trans.* (1995) 47: 213–237.
[3] Khan, A.S. and Huang, S. *Continuum Theory of Plasticity*. New York (1995).
[4] Kobayashi, S. and Oh, S.I. and Altan, T. *Metal Forming and the Finite Element Method*. Oxford University (1989).
[5] Lou, S. and Zhao, G. and Wang, R. and Wu, X. Modeling of aluminum alloy profile extrusion process using finite volume method. *Journ. of Mat. Proc. Tech.* (2008) 206: 481–490.
[6] Maliska, C.R. *Transferência de Calor e Mecânica dos Fluidos Computacional*. LCT (2004).
[7] Malvern, L.E. *Introduction to the Mechanics of a Continuous Medium*. Prentice-Hall (1969).
[8] Martins, P. and Rodrigues, J. *Tecnologia Mecânica: tecnologia da deformação plástica; fundamentos teóricos*. Escolar, Vol I (2005).
[9] Mielnik, E. *Metalworking Science and Engineering*. McGraw-Hill (1991).
[10] Rhie, C.M. and Chow, W.L. "A Numerical Study of the Turbulent Flow Past an Isolated Airfoil with Trailing Edge Separation". *Am. Inst. of Aero. and Astron.* (1983) 21: 1525-1532.
[11] Tannehill, J.C. and Anderson, D.A. and Pletcher, R.H. *Computational Fluid Mechanics and Heat Transfer*. Taylor&Francis (1997).
[12] Valberg, H.S. *Applied Metal Forming: Including FEM Analysis*. Cambridge University Press (2010).
[13] Williams, A.J. and Croft, T.N. and Cross, M. Computational modeling of metal extrusion and forging processes. *Journ. of Mat. Proc. Tech.* (2002) 125-126: 573–582.
[14] Zdanski, P.S.B. and Vaz Jr, M. and Inácio, G.R. A Finite Volume Approach to Simulation of Polymer Melt Flow in Channels. *Eng. Comp*. (2008) 25: 233-250.
[15] JASAK, H. *Error Analysis and Estimation for the Finite Volume Method with Applications to Fluid Flows.* Thesis (Doutorado) – Department of Mechanical Engineering, Imperial College of Science, Technology and Medicine, London, (1996).